Belt and Altgen *J Mater. Sci: Mater Eng.* (2025) 20:19
https://doi.org/10.1186/s40712-025-00228-5

Journal of Materials Science: Materials in Engineering

ORIGINAL PAPER

Open Access

Changes in wood-water relations in acetylated wood over the course of *Rhodonia placenta* brown rot decay

Tiina Belt[1*] and Michael Altgen[2]

Abstract

Acetylation greatly increases the decay resistance of wood, but even highly acetylated wood can be degraded by fungi if given sufficient time. This study investigated the degradation of acetylated wood by the brown rot fungus *Rhodonia placenta*, aiming to understand the fungal-induced changes in wood-water relations that are associated with decay. Acetylated samples as well as unacetylated references were exposed to *R. placenta* in a stacked-sample decay test to generate samples in different stages of decay. The decayed samples were used to investigate changes in acetyl content, water vapour sorption, and maximum cell wall moisture content as measured by solute exclusion. *R. placenta* caused high mass losses in acetylated wood, but preferential deacetylation was seen only in highly acetylated samples in the early stages of decay. Acetylated samples showed increased hygroscopicity in sorption measurements as a result of *R. placenta* degradation, particularly at high relative humidity in desorption from the undried decaying state. The increase was very strong in the highly acetylated samples and took place at low mass losses, indicating that it may be at least partially related to the deacetylation of the wood material. Degradation also increased maximum cell wall moisture content, but the increase was stronger in the references than the acetylated samples, suggesting that the acetyl groups remaining in the samples continue to provide a cell wall bulking effect.

Keywords Acetylation, Anhydride, Brown rot, Decay, Durability, Dynamic vapour sorption, Hygroscopicity, Moisture, Solute exclusion, Wood modification

Introduction

As a natural material, wood is susceptible to degradation by many abiotic and biotic agents, including wood-decaying fungi. Wood-decaying fungi are highly specialised and destructive wood degraders that depolymerise and consume the structural wood cell wall polymers, weakening the material and structures made therefrom. Many methods have been developed to protect susceptible wood from decay, including several different types of wood modification (Sandberg et al. 2021). Acetylation is an extensively studied wood modification method that was developed in the 1940s for dimensional stabilisation (Sandberg et al. 2021). It uses acetic anhydride to replace accessible OH groups on the wood cell wall polymers with acetyl esters, which greatly increases the decay resistance of the wood material (Alfredsen et al. 2013).

The mechanisms behind the increased decay resistance of acetylated and other modified woods have been extensively studied, and it has been demonstrated that the increase is due to a permanent reduction in the moisture content of the wood cell walls (Thybring 2013; Ringman et al. 2014, 2019; Zelinka et al. 2016). Acetylation reduces moisture content throughout the hygroscopic (Papadopoulos and Hill 2003; Popescu et al. 2014; Himmel and Mai 2015; Čermák et al. 2022;

*Correspondence:
Tiina Belt
tiina.belt@luke.fi
[1] Production Systems Unit, Natural Resources Institute Finland, Viikinkaari 9, 00790 Helsinki, Finland
[2] Department of Wood Technology, Norwegian Institute of Bioeconomy Research, P.O. Box 115, 1431 Ås, Norway

Awais et al. 2022) and overhygroscopic (Thygesen et al. 2010; Fredriksson et al. 2023) moisture range and at full water saturation (Hill et al. 2005; Beck et al. 2018c; Digaitis et al. 2021). The reduction is primarily due to cell wall bulking (Papadopoulos and Hill 2003; Thybring et al. 2020b), i.e. the pre-swelling of the cell walls by the added acetyl groups which reduce the space available for water molecules. It is thought that the reduced moisture content protects wood from decay because it hinders the diffusion of fungal degradative agents in the cell walls (Ringman et al. 2014, 2019; Zelinka et al. 2016). Wood decaying fungi utilise diffusible small molecular degradative agents particularly in the early stages of decay (Hammel et al. 2002; Arantes and Goodell 2014; Daniel 2014), which means that the reduction in moisture content is expected to hinder the initiation of decay.

Even though acetylated wood can have very high decay resistance, studies utilising longer decay test times have shown that even highly acetylated wood can eventually be degraded (Hill et al. 2006; Beck et al. 2018b, 2018a; Thygesen et al. 2021; Ponzecchi et al. 2024; Belt and Awais 2025). The degradation of acetylated wood suggests that the wood-decaying fungi can either eliminate the moisture exclusion effect caused by the modification or degrade the wood despite the reduced moisture content. Recent studies have revealed that the brown rot fungus *Rhodonia placenta* can deacetylate acetylated wood (Beck et al. 2018b; Ponzecchi et al. 2024; Belt and Awais 2025), providing a means for the fungus to eliminate the moisture-excluding bulking effect. Acetylated wood degraded by *R. placenta* showed a rapid increase in moisture content at low mass losses, coinciding with the deacetylation recorded at low mass losses (Belt and Awais 2025). The initial deacetylation and the increase in moisture content suggest that deacetylation plays a role in the initiation of decay. However, only partial deacetylation by *R. placenta* has been recorded (Beck et al. 2018b; Ponzecchi et al. 2024; Belt and Awais 2025), which suggests that complete deacetylation is not necessary and that a moisture content sufficiently high for decay can be reached even in the presence of acetyl groups.

To better understand the degradation of acetylated wood, this study investigated the changes in wood-water relations in acetylated wood over the course of brown rot decay by *R. placenta*. Acetylated samples and unacetylated references previously exposed to *R. placenta* in a stacked-sample decay test (Belt and Awais 2025) were used for sorption isotherm and solute exclusion measurements to analyse changes in cell wall moisture content in the hygroscopic range and at full saturation. The acetyl contents of the samples after decay were measured by saponification to correlate potential changes in wood-water relations with changes in acetyl content.

Materials and methods

Sample preparation

The samples and the decay test were part of the previously reported experiment (Belt and Awais 2025). The samples were Scots pine (*Pinus sylvestris*) sapwood blocks sized 8×8×12 mm (L×T×R) that were prepared from commercial boards with an average density of approx. 515 kg/m^3 and were free of knots and any visible defects. The samples were acetylated to two different treatment levels or left untreated to act as references. All samples were first Soxhlet extracted with acetone and then dried at 105 °C for 24 h to determine their initial dry mass, after which the samples to be acetylated were impregnated with neat acetic anhydride at room temperature (2 h under vacuum, overnight soaking at atmospheric pressure). Acetylation was performed in fresh anhydride at 120 °C for 20 min or 6 h. After acetylation, the anhydride was replaced with acetone, and the acetylated samples were again Soxhlet extracted with acetone, then dried at 105 °C for 24 h to determine their modified dry mass. Weight percent gain (WPG) due to modification was calculated according to Eq. 1,

$$WPG(\%) = \frac{m_{\mathrm{mod}} - m_{\mathrm{init}}}{m_{\mathrm{init}}} \times 100\% \quad (1)$$

where m_{mod} is the modified dry mass, and m_{init} is the initial dry mass.

After treatment, the acetylated and reference samples were sterilised by ionising radiation (25–50 kGy dose) and conditioned for 3 months at 85% RH over a saturated solution of KCl.

Decay test

The decay test was a stacked-sample test performed in test tubes over malt extract agar (Belt and Awais 2025). The agar in each tube was inoculated with a plug of *R. placenta* (strain BAM 113, Federal Institute for Materials Research and Testing, Germany) mycelium cut from the growing edges of stock cultures maintained on malt extract agar. A piece of polyethylene plastic netting was placed over the inoculated agar, followed by six samples stacked on top of each other (see Fig. 3). Seven replicate tubes were prepared for each sample type. The tubes were plugged with cotton wool and incubated at 85% RH at room temperature over a saturated solution of KCl. Different test durations were used for the different sample types, with all replicate tubes corresponding to one sample type removed once the visible mycelial front reached the top of the topmost block in one replicate tube. The samples were removed from the tubes, wiped

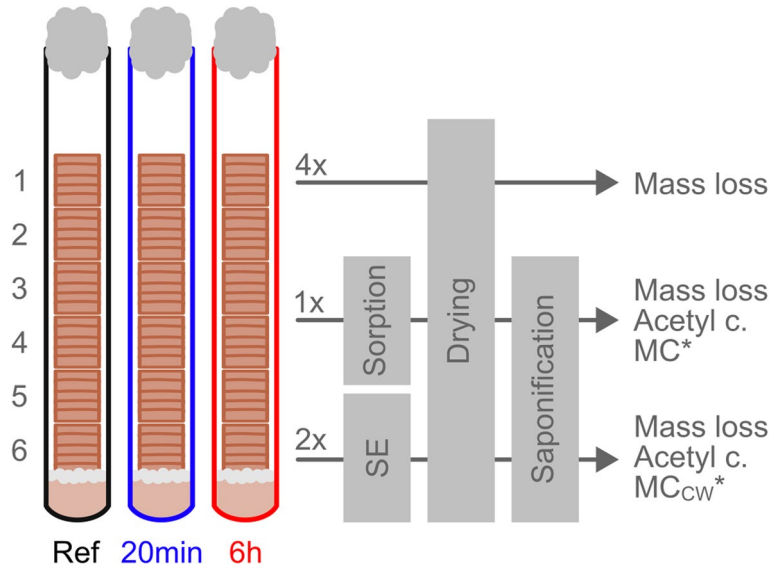

Fig. 1 Reference and acetylated (20 min or 6 h) samples were exposed to *R. placenta* in a stacked-sample decay test. Sample positions were numbered 1–6 as indicated. Four replicate tubes of decayed samples were dried to determine their mass loss, while one tube was used for sorption measurements and two tubes for solute exclusion (SE) measurements. The sorption and SE samples were dried after measurement to determine their mass loss and then saponified to determine their post-decay acetyl content, which was used to calculate corrected moisture content (MC*) for the sorption data and corrected maximum cell wall moisture content (MC_{CW}*) for the SE data

to remove attached mycelium, and weighed to determine their decaying mass. Samples belonging to three of the seven replicate tubes were packed in sealed plastic tubes and stored frozen at − 20 °C until further analysis. The samples belonging to the remaining tubes were dried (overnight at room temperature, then 24 h at 105 °C), and their decayed dry masses were measured. Mass loss (Δm) due to decay was calculated according to Eq. 2,

$$\Delta m(\%) = \frac{m_{\mathrm{undec}} - m_{\mathrm{dec}}}{m_{\mathrm{undec}}} \times 100\% \quad (2)$$

where m_{undec} is the initial dry mass for the unmodified reference samples or the modified dry mass for the modified samples, and m_{dec} is the decayed dry mass. The decay test setup and the following analyses are summarised in Fig. 1.

Water vapour sorption

One of the three frozen replicate tubes was selected for sorption isotherm measurements. The samples were vacuum impregnated with water approx. 24 h before measurement and then placed on the sample cups of the automated sorption balance (Vsorp Enhanced, ProUmid, Germany) for simultaneous water vapour sorption measurements. One of the sample cups in the sample carousel was kept empty to correct for balance drift, and one was filled with ca. 115 mg of a non-hygroscopic material (aluminium Differential Scanning Calorimetry (DSC) sample pans) to record the mass. Each cup was weighed at 15-min intervals. The samples were conditioned at RH steps of 90, 80, 70, 60, 50, 40, 30, 20, 10, and 0% in desorption from the undried, decaying state, followed by conditioning using the same RH steps in reverse order in absorption from the dried state. Each RH step was held until the sample mass change was less than 0.01% for all samples, calculated based on the slope of a linear regression line within a 60-min time window that moved forward with each weighing step. The average sample mass within this moving time window was used as reference mass. The mass changes measured at the end of each RH step were close to the |3| µg g^{-1} min^{-1} mass stability criterion recommended by Glass et al. (2018) as shown in Supplementary Figure S1. Finally, the samples were exposed at 0% RH and 40 °C for 48 h to determine their dry mass. The average sample mass during the final hour of this step was used as the reference mass to calculate the moisture content (MC) of each sample according to Eq. 3,

$$MC(\%) = \frac{m_{\mathrm{RH}} - m_{\mathrm{dry}}}{m_{\mathrm{dry}}} \times 100\% \quad (3)$$

where m_{RH} is the average sample mass during the final hour of each RH step, and m_{dry} is the average sample mass during the final hour of the drying step.

The mass stability of the sorption balance was shown by the 24-h slope of the inert sample, which did not exceed |0.47| µg day^{-1}, see Supplementary Fig. S2. This was nearly one magnitude lower than the tentative mass

stability target of 4 µg day^{-1} applied by Zelinka et al. (2024).

After measurement, the samples were dried at 105 °C for 24 h and weighed to measure their decayed dry mass. Mass loss was calculated according to Eq. 2.

Solute exclusion

The remaining two frozen replicate tubes were used to measure maximum cell wall moisture content by the solute exclusion technique using a modified version of previously reported methods (Flournoy et al. 1991; Thybring et al. 2020a). The samples were first split in two lengthwise along the L-R plane using a razor blade, after which one-half from each sample was saturated with ultrapure water. The other half was dried (overnight at room temperature, then 24 h at 105 °C), weighed to determine its initial dry mass, and then saturated with ultrapure water. Both saturated sample halves were leached in ultrapure water for 1 week (water changed every 1–3 days), followed by 2 weeks of incubation in a solution with 0.05% NaN_3 as antimicrobial agent (solution changed after 1 week). The sample halves were removed from the NaN_3 solution, dabbed with a moist tissue to remove excess solution, and moved to 3 ml cryotubes. Each tube received 0.6 ml of a solution containing 1% dextran (average molecular weight 43.2 k, Sigma) as the solute exclusion probe and 0.05% NaN_3. The high-molecular-weight dextran has an average diameter of 10.7 nm as calculated according to Thybring et al. (2018), which means that it is unable to enter the wood cell wall (Flournoy et al. 1991; Hill et al. 2005; Thybring et al. 2018). The tubes were incubated at room temperature for 2 weeks to allow the dextran probe to enter the cell lumens and reach equilibrium. An aliquot of the initial probe solution was also stored under the same conditions for 2 weeks without wood. After incubation, the solution in each tube was collected, filtered into HPLC vials through 0.45 µm syringe filters, and analysed by HPLC using refractive index detection on a Shimadzu Prominence system (consisting of a LC-20AP pump, SIL-20AC autosampler, CTO-20AC column oven, and RID-10A refractive index detector) using a Waters XBridge C18 column (4.6×150 mm, 5 µm particle size) and isocratic elution with 10% acetonitrile as the mobile phase at 1 ml min^{-1}. After removal of the probe solution, the wood sample halves were leached in ultrapure water for 2 weeks (water changed every 1–3 days) to remove the dextran and NaN_3. The sample halves were then dabbed with a moist tissue to remove excess water and weighed to determine their water-saturated mass as an average of four measurements. Finally, the sample halves were dried (overnight at room temperature, then 24 h at 105 °C) and weighed to determine their final dry mass. The initial and final dry masses of the sample half that was dried before water saturation were used to calculate a leaching factor (L) according to Eq. 4,

$$L = \frac{m_{h,\mathrm{init}} - m_{h,\mathrm{final}}}{m_{h,\mathrm{init}}} \tag{4}$$

where $m_{\mathrm{h,init}}$ is the initial dry mass of the sample half, and $m_{\mathrm{h,final}}$ is the final dry mass of the sample half.

The mass loss of the whole sample due to decay (Δm) was then estimated according to Eq. 5,

$$\Delta m(\%) = \frac{m_{h,\mathrm{init},1} + m_{h,\mathrm{final},2} \times (1+L)}{m_{\mathrm{undec}}} \times 100\% \tag{5}$$

where $m_{\mathrm{h,init,1}}$ is the initial dry mass of the sample half that was dried before water saturation, $m_{\mathrm{h,final,2}}$ is the final dry mass of the sample half that was not dried before water saturation, L is the leaching factor, and m_{undec} is the undecayed dry mass of the whole sample (initial dry mass for the unmodified reference samples, the modified dry mass for the modified samples).

Maximum cell wall moisture content (MC_{CW}) was calculated for each sample half according to Eq. 6,

$$MC_{CW}(\%) = \frac{m_{h,WS} - m_{h,\mathrm{final}} - m_{\mathrm{sol}} \times \left(\frac{C_{\mathrm{init}}}{C_s} - 1\right)}{m_{h,\mathrm{final}}} \times 100\% \tag{6}$$

where $m_{\mathrm{h,WS}}$ is the average water-saturated mass of the sample half, $m_{\mathrm{h,final}}$ is the final dry mass of the sample half, m_{sol} is the mass of the added probe solution, C_{init} is the HPLC peak area of initial probe solution, and C_s is the HLC peak area of the probe solution incubated with the sample half.

Saponification

After sorption and maximum cell wall moisture content measurements, the dried samples were ground to fine powder in a laboratory mill (MC_{CW} sample halves combined). The acetyl content of the samples was determined by saponification as previously described (Belt and Awais 2025). Briefly, 25 mg of sample was saponified with 1 ml of 1 M NaOH for 6 h on a flatbed shaker, after which 0.75 ml of the fluid was collected, neutralised with 0.375 ml of 2 M HCl, and filtered into HPLC a vial through a 0.45 µm syringe filter. Acetic acid content was determined by HPLC using refractive index detection on a Shimadzu Prominence system (consisting of a LC-20AP pump, SIL-20AC autosampler, CTO-20AC column oven, and RID-10A refractive index detector) equipped with a Phenomenex Rezex ROA-Organic Acid H+column (7.8×300 mm, 8 µm particle size) at 55 °C using 2.5 mM H_2SO_4 as the mobile phase at 0.6 ml min^{-1}. Acetic acid was quantified against a calibration curve of acetic acid standards prepared in the same way as the samples.

The post-decay acetyl content of each sample was used to calculate corrected moisture content (MC*) values for the sorption isotherm data according to Eq. 7,

$$MC^*(\%) = MC \times (1 + a) \tag{7}$$

where MC is the moisture content calculated according to Eq. 3, and a is the acetyl content (g g^{-1}) determined by saponification.

The post-decay acetyl content was also used to calculate corrected maximum cell wall moisture content (MC_{CW}*) values for the solute exclusion data according to Eq. 8,

$$MC^*_{CW}(\%) = MC_{CW} \times (1 + a) \tag{8}$$

where MC_{CW} is the cell wall moisture content calculated according to Eq. 6, and a is the acetyl content (g g^{-1}) determined by saponification.

Results

Mass loss and acetyl content

The Scots pine sapwood samples acetylated for 20 min or 6 h reached average WPGs of 9.3 ± 0.8% and 18.3 ± 0.5%, respectively. The acetylated samples and unmodified references were exposed to *R. placenta* in a stacked-sample decay test as previously reported (Belt and Awais 2025). The average mass losses of all replicate samples are given in Fig. 2a, including the solute exclusion samples whose mass losses were estimated after measurement. The mass losses of the individual samples selected for sorption and solute exclusion measurements are given in Fig. 2b. As the objective of the decay test was to produce a range of mass losses, the three different sample types were exposed to *R. placenta* until the visible fungal mycelium reached the top of the topmost sample in one replicate tube. The reference samples were fully colonised in 14 weeks, while the WPG-9 and WPG-18 samples were colonised in 26 and 52 weeks, respectively. The reference samples showed a non-linear increase in mass loss from -1.5% at position 1 to 51.8% at position 6. The WPG-9 samples produced a very similar pattern of mass losses, while the WPG-18 samples showed little mass loss up to position 4, followed by a rapid increase to 40.4% at position 5 and 48.4% at position 6. The mass losses of the samples selected for sorption and solute exclusion measurements corresponded well with the average mass losses.

The post-decay acetyl contents of the sorption and solute exclusion samples are presented in Fig. 3. The results agree with the data obtained for other samples derived from the same decay test (Belt and Awais 2025). The reference samples had a low concentration of acetyl groups (0.016–0.019 g g^{-1} in the least degraded samples) due to the natural acetylation of native wood hemicelluloses (Fengel and Wegener 1989). The acetyl content of the references decreased linearly with increasing mass loss. The acetylated samples showed substantial variation in their acetyl content, most likely due to variation in their acetylation degree: the gravimetrically determined WPGs of the selected WPG-9 samples ranged from 8.0 to 10.5%, while the WPGs of the selected WPG-18 samples ranged from 17.9 to 19.3%. The WPG-9 samples showed no change in acetyl content as a function of mass loss, suggesting that no preferential deacetylation took place and that acetyl groups were lost from the samples

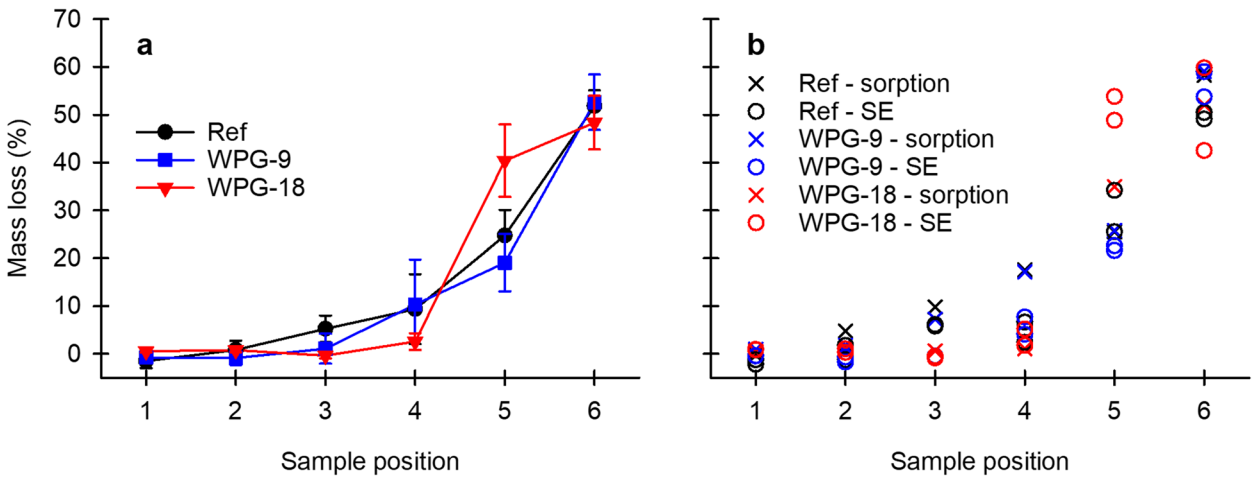

Fig. 2 Average mass loss of all replicate reference and acetylated (WPG-9 and WPG-18) samples (**a**) and mass loss of individual samples selected for sorption and solute exclusion (SE) measurements (**b**) as a function of sample position in the decay test. The reference, WPG-9, and WPG-18 samples were exposed to *R. placenta* for 14, 26, and 52 weeks, respectively. Error bars in **a** are ± SD ($N = 7$). The mass losses of the solute exclusion samples were estimated according to Eq. 5, while the rest were calculated according to Eq. 2

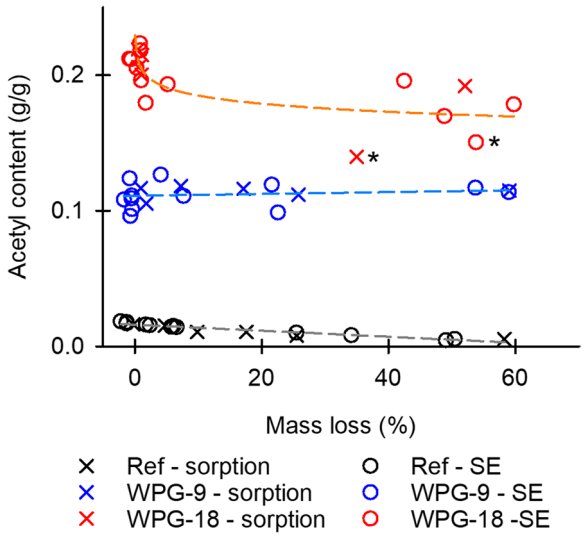

Fig. 3 Post-decay acetyl contents of the reference and acetylated (WPG-9 and WPG-18) samples selected for sorption and solute exclusion (SE) measurements as a function of mass loss. Two WPG-18 samples with reduced acetyl content are marked with asterisks (*)

at the same rate as cell wall polymers. The WPG-18 samples on the other hand revealed a small but noticeable decrease in acetyl content at low mass losses, indicating that *R. placenta* caused preferential deacetylation of high WPG acetylated wood in the early stages of decay. Most of the WPG-18 samples showed no further deacetylation at high mass losses; however, two samples (marked with asterisks in Fig. 5) were found to have noticeably reduced acetyl content. This finding suggests that further deacetylation may happen in more advanced decay, but mostly acetyl groups are lost from the material at the same rate as cell wall polymers.

Water vapour sorption isotherms

Sorption isotherms were measured for the reference and acetylated samples starting in desorption from the undried state to understand how decay affects hygroscopicity. Sorption isotherms plotted using acetyl-corrected moisture content (MC*) are given in Fig. 4a for the position 1 (least decayed) samples and in Fig. 4b for the position 6 (most decayed) samples. All measured isotherms can be found in Supplementary Fig. S3. MC* ratios of the position 1 samples relative to the position 1 reference are given in Fig. 4c to show the effects of acetylation, while the MC* ratios of the position 6 samples relative to the corresponding position 1 samples are given in Fig. 4d to show the effects of decay. The position 1 samples (Fig. 4c) showed that acetylation reduced the hygroscopicity of wood in the whole hygroscopic range. However, the

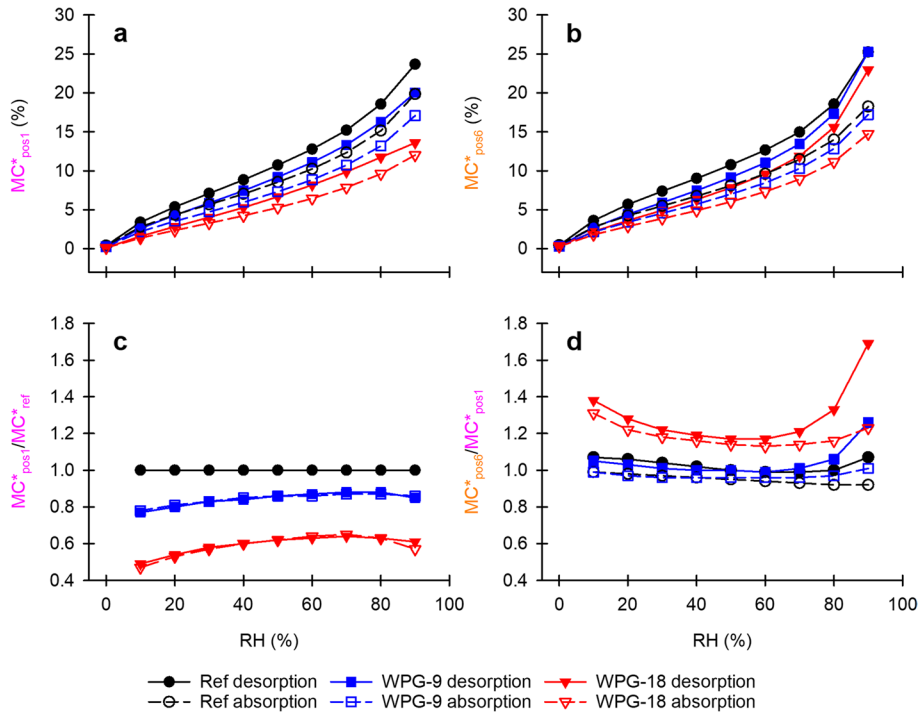

Fig. 4 Sorption isotherms of position 1 (least decayed) (**a**) and position 6 (most decayed) (**b**) reference and acetylated (WPG-9 and WPG-18) samples plotted using acetyl-corrected moisture content (MC*) in desorption from the undried state and absorption from the dry state, and MC* ratios of the position 1 samples relative to the position 1 reference (**c**) and the position 6 samples relative to the corresponding position 1 samples (**d**). The mass losses of the position 6 reference, WPG-9, and WPG-18 samples were 58.3%, 59.1%, and 52.0%, respectively

effect was stronger at low RH. The position 6 samples (Fig. 4d) revealed that decay affected the different sample types in different ways. The position 6 references showed a small increase in MC* at high and low RH in desorption and a small decrease with increasing RH in absorption compared to the position 1 references. The WPG-9 samples showed an increase in MC* at high RH in desorption but little change at any RH in absorption. The WPG-18 samples on the other hand revealed an increase in MC* throughout the hygroscopic range in both desorption and absorption. The increase was strong at low RH in both desorption and absorption and very strong at high RH in desorption.

Wood-water relations as a function of mass loss

To better understand the effects of decay on the different sample types, the changes in wood-water relations were examined as a function of mass loss. MC* at 90% RH was used to explore changes in hygroscopicity in the high RH range relevant for decay, while the maximum cell wall moisture content (MC_{CW}*) determined by solute exclusion was used to examine changes in cell wall water capacity. Figure 5 gives the MCs* in desorption from the undried state (Fig. 5a) and absorption from the dry state (Fig. 5b), and the MC_{CW}* values measured before (Fig. 5c) and after drying (Fig. 5d). In desorption from the undried state, MC* generally increased with mass loss. The references showed a slight increase in MC* until 25% mass loss, followed by a small decrease at very high mass loss. The acetylated samples in turn showed a rapid increase in MC* at low mass loss, followed by a more gradual increase with further mass loss similar to the references. The initial increase in MC* was much stronger in the WPG-18 samples than in the WPG-9 samples, although the difference may be at least partially due to differences in the number of low mass loss samples. The two WPG-18 samples with high mass loss showed little difference in their MC*; however, the sample with 35% mass loss had reduced post-decay acetyl content (0.14 g g^{-1} compared to > 0.19 in the other samples), which is likely to have caused an increase in its MC*. In absorption from the dry state, the MC* of the reference samples decreased linearly with mass loss, while the acetylated samples showed an initial increase in MC* at low mass loss, followed by a plateau at higher mass losses.

MC_{CW}* was affected by both acetylation and decay. Acetylation reduced the average MC_{CW}* of the position 1 samples from 42.4% in the references to 39.0% in the WPG-9 samples and to 24.5% in the WPG-18 samples when measured before drying (Fig. 5c). Decay increased MC_{CW}* in all samples measured before drying (Fig. 5c). The MC_{CW}* of the references increased almost linearly with mass loss and reached 86.6% in the most decayed sample with 50.4% mass loss. The WPG-9 samples also showed a linear increase in MC_{CW}* with mass loss. However, MC_{CW}* increased more slowly in the WPG-9

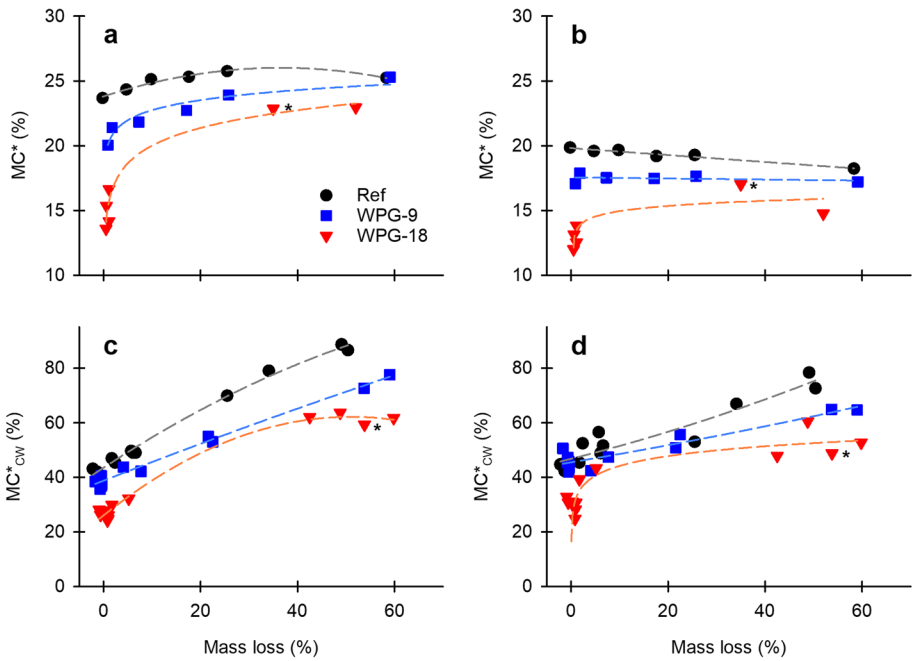

Fig. 5 Acetyl-corrected moisture content (MC*) at 90% RH in desorption from the undried state (**a**) and in absorption from the dried state (**b**), and acetyl-corrected maximum cell wall moisture content (MC_{CW}*) measured before drying (**c**) and after drying (**d**) of the reference and acetylated (WPG-9 and WPG-18) samples as a function of mass loss. WPG-18 samples with reduced acetyl content are marked with an asterisk (*)

samples than in the references and reached only 77.6% in the sample with 59.0% mass loss. The WPG-18 samples on the other hand showed an initial increase in MC_{CW}^* with mass loss, followed by a plateau at higher mass losses. Decay increased MC_{CW}^* also in all samples measured after drying (Fig. 5d), but the scatter in the data was higher. The dried reference and WPG-9 samples showed similar trends as the undried samples, but the MC_{CW}^* values were lower, indicating that a portion of the cell wall water capacity had been permanently lost on drying. The dried WPG-18 samples showed a rapid initial increase in MC_{CW}^* at low mass losses that was not seen in the undried samples. The differences in the behaviour of the WPG-18 samples may be due to the higher data scatter, or they may indicate that the WPG-18 samples respond to drying differently than the other samples.

Discussion

As previously reported (Belt and Awais 2025), the stacked-sample decay test showed that acetylation increased the sample colonisation time by *R. placenta* from 14 weeks in the references to 26 weeks in the WPG-9 samples and to 52 weeks in the WPG-18 samples. The reference and WPG-9 samples showed a similar non-linear increase in mass loss with sample position, while the WPG-18 samples showed little mass loss until position 4, followed by a rapid increase in mass loss (Fig. 2). As before, the mass loss results demonstrated that even high WPG acetylated wood can be degraded over time, confirming the findings of previous long-duration decay tests (Hill et al. 2006; Beck et al. 2018a, 2018b; Thygesen et al. 2021; Ponzecchi et al. 2024).

The WPG-9 samples showed no change in acetyl content with mass loss, while the WPG-18 samples revealed a small but noticeable decrease at low mass losses (Fig. 3) in agreement with the results reported for other samples derived from the same decay test (Belt and Awais 2025). Deacetylation of high WPG wood by *R. placenta* has been previously documented (Beck et al. 2018b; Ponzecchi et al. 2024), and it has been shown that the deacetylation takes place in the early stages of decay (Beck et al. 2018b). The results presented here are in agreement, although the extent of deacetylation was lower than previously observed (Beck et al. 2018b). The initial deacetylation may be caused by the targeted removal of acetyl groups or by the action of the oxidative Fenton reaction-based degradative system that brown rot fungi utilise in incipient decay (Arantes and Goodell 2014). The acetyl content data does not reveal which mechanism is involved, but the initial deacetylation appears to be specific to the WPG-18 samples. Apart from the initial deacetylation of the WPG-18 samples, the acetyl content of the WPG-9 and WPG-18 samples remained constant over the course of decay, indicating that the acetyl groups were lost from the samples at the same rate as wood cell wall polymers. Extensive deacetylation does not appear to be necessary for the degradation of acetylated wood, although the lack of preferential deacetylation in the bulk measurement data does not rule out the possibility on a more localised scale. Ponzecchi et al. (2024) found no differences in deacetylation on the cell level in acetylated wood degraded by *R. placenta*, but their results revealed reduced carbohydrate degradation in regions with a higher degree of acetylation.

The sorption measurements (Fig. 4) showed that acetylation reduced the hygroscopicity of the samples in the whole hygroscopic range. The effect was stronger at low RH (Fig. 4c), as has been previously documented for acetylated wood (Himmel and Mai 2015; Awais et al. 2022). Decay affected the sorption isotherms in all three sample types but in different ways and to different extents. The most decayed reference showed only small changes in MC* at any given RH in desorption or absorption relative to the least decayed reference (Fig. 4d), in contrast to previous results (Belt et al. 2024), which revealed a notable increase in MC in the unmodified references in desorption at 90% RH. The most decayed WPG-9 sample showed increased MC* at high RH in desorption relative to the least degraded sample (Fig. 4d) but little change at low RH or any RH in absorption. The most decayed WPG-18 sample in turn showed increased MC* throughout the hygroscopic range in both desorption and absorption. The increase was strong at low RH in both desorption and absorption, and very strong at high RH in desorption. The increase in MC* suggests that *R. placenta* decay can eliminate the decrease in moisture content caused by acetylation, which is thought to give rise to the decay resistance of acetylated wood (Thybring 2013; Ringman et al. 2014, 2019; Zelinka et al. 2016). The increase in MC* at high RH is particularly relevant for decay. A similar increase in desorption MC* at high RH has been observed in heat-treated wood (Belt et al. 2024), which also has increased decay resistance due to reduced hygroscopicity (Thybring 2013; Ringman et al. 2014, 2019). The strong increase in the MC* of the most decayed sample at low RH is most likely because acetylation caused a strong reduction in MC* at low RH (Fig. 4c); the elimination of the acetylation-related hygroscopicity decrease is therefore likely to increase MC* particularly at low RH.

The effects of decay on wood-water relations were examined by plotting MC* at 90% RH and MC_{CW}^* as a function of mass loss (Fig. 5). MC* at 90% RH in desorption increased with mass loss in all sample types, but only the acetylated samples showed a rapid increase at low mass losses (Fig. 2a). The increase was very strong

in the WPG-18 samples and coincided with the initial deacetylation (Fig. 3), which suggests that the rapid increase in hygroscopicity may be caused by the removal of acetyl groups. However, deacetylation is not the only factor contributing to the increase in MC* with decay, given that an increase was seen also in the reference and WPG-9 samples in desorption. The more modest and gradual increase in MC* seen in these samples is likely due to other cell wall alterations caused by brown rot degradation. Brown rot fungi preferentially degrade the cell wall carbohydrates and leave behind a skeleton of modified lignin (Curling et al. 2002; Filley et al. 2002; Yelle et al. 2011). The degradation takes place by a diffusible mechanism, which involves the degradation of the cell wall polymers in situ and the diffusion of depolymerised carbohydrate fragments out of the cell wall (Goodell et al. 2017; Zhu et al. 2022). The removal of carbohydrates creates space in the cell wall and is likely to promote increased water sorption at high RH. Increased water sorption as a result of carbohydrate removal has been demonstrated on pressurised hot water extracted wood (Kyyrö et al. 2021). The increased cell wall space collapses on drying (Kyyrö et al. 2021), which likely explains why the MC* of the reference samples increased in desorption from the decaying state but decreased in absorption from the dry state (Fig. 5b). The degradation of carbohydrates is likely to cause a further decrease in hygroscopicity, although some of the chemical alterations may also serve to increase hygroscopicity (Belt et al. 2024).

MC_{CW}* measured by solute exclusion decreased with acetylation and increased with mass loss. When measured before drying (Fig. 5c), the MC_{CW}* of the least decayed references (42%) was similar to the cell wall saturation value obtained by solute exclusion for Norway spruce (Thybring et al. 2020a) and Corsican pine (Hill et al. 2005), while the reduced values of acetylated wood (39% for WPG-9 and 25% for WPG-18) were similar to those obtained by Hill et al. (2005). The reference MC_{CW}* increased almost linearly with mass loss to a maximum of 89% MC_{CW}* at 49% mass loss when measured before drying (Fig. 5c), which is similar to previous solute exclusion results that found an increase in MC_{CW} from 35% before degradation to 70% at 35% mass loss due to *R. placenta* (Flournoy et al. 1991). An increase in MC_{CW}* is expected with brown rot decay because the removal of carbohydrates from the cell wall creates new water-accessible space. However, a non-linear relationship was found when the measured increase in MC_{CW}* was plotted against an expected increase calculated assuming that the lost cell wall mass was completely replaced by water (see Supplementary Figure S4). The measured reference MC_{CW}* increased at approximately the expected rate until around 30% mass loss when measured before drying, after which the measured increase fell behind the expected increase (Supplementary Fig. S4a). The reduced increase in MC_{CW}* at high mass losses suggests that not all removed cell wall mass creates water-accessible space or that there is a loss of cell wall volume due to erosion or shrinkage. Cell wall shrinkage is likely to at least contribute to the reduced increase given that the extensively degraded samples showed visible shrinkage in their external dimensions.

Like the references, the WPG-9 samples also showed a mostly linear increase in MC_{CW}* with mass loss. However, the rate of increase was lower than in the references (Fig. 5c) and fell below the expected rate of increase at lower mass losses (Supplementary Fig. S4a). These differences indicate that the removal of cell wall polymers creates less space available for water in the WPG-9 samples than the references. It is unclear if the WPG-9 cell wall material undergoes more shrinkage or if some other mechanism is involved. The WPG-18 samples showed an initial increase in MC_{CW}* with mass loss and a plateau at higher mass losses (Fig. 5c, Supplementary Fig. S4a). Although the WPG-18 samples showed a different MC_{CW}* pattern than the WPG-9 samples, the data indicate that the removal of cell wall polymers creates less space available for water in the WPG-18 samples as well, particularly at high mass losses. The WPG-18 samples did not show a rapid increase in MC_{CW}* at low mass loss when measured before drying, which suggests that MC_{CW}* is not as strongly affected by deacetylation as MC* at 90% RH. The WPG-18 samples measured after drying (Fig. 5d) showed an increase at low mass losses, but it is unclear if this reflects real behaviour or if it is due to high data scatter. However, it is clear that acetylation degree has an overall influence on the MC_{CW}* and that the acetyl groups remaining in the samples continue to provide a bulking effect as decay advances, keeping the water capacity of the cell walls lower than in the references at comparable mass loss.

Plotting MC* at 90% RH and MC_{CW}* as a function of mass loss revealed that hygroscopicity and cell wall water capacity were affected by decay in different ways. Hygroscopicity seemed to be strongly affected by deacetylation and slightly affected by the degradation of cell wall polymers. The strong influence of deacetylation on hygroscopicity is not surprising, given that the MC* of acetylated wood in the hygroscopic range has been shown to decrease as a function of the added acetyl content (Thybring 2013; Popescu et al. 2014; Thybring et al. 2020b). The reduced moisture content is thought to interfere with the diffusion of fungal degradative agents (Ringman et al. 2014, 2019; Zelinka et al. 2016), and the removal of a portion of the acetyl groups may be necessary for *R. placenta* decay to allow the moisture content

of the cell walls to increase to a level where sufficient diffusion is possible. Cell wall water capacity on the other hand seemed to be more strongly affected by the degradation of cell wall polymers, even if the measured MC_{CW}^* values were often below the expected values. The samples measured before drying showed no clear effect from deacetylation, while the samples measured after drying showed an effect that may or may not be a consequence of higher data scatter in the measurement. The uncertain and lacking influence of deacetylation on MC_{CW}^* is unexpected since the relationship between moisture at saturation and the added acetyl content has been previously demonstrated in undegraded wood (Hill et al. 2005; Thybring 2013; Beck et al. 2018c) and was also visible in this experiment in the MC_{CW}^* values of the least degraded samples (Fig. 5c,d). It is possible that the effects of deacetylation on MC_{CW}^* were masked by the stronger effect of cell wall polymer degradation or increasing shrinkage of the cell wall material.

Conclusions

Acetyl content measurements showed that extensive deacetylation is not a requirement for the degradation of acetylated wood, with preferential deacetylation taking place only in the WPG-18 samples in the early stages of decay. *R. placenta* degradation caused a strong increase in the hygroscopicity of the WPG-18 samples in early decay, which suggests that the hygroscopicity increase may be connected to deacetylation. However, other factors are also likely to contribute to the increased hygroscopicity as evidenced by the fact that the reference and WPG-9 samples showed a smaller increase despite no deacetylation. The MC_{CW}^* of the acetylated samples increased with decay, but the increase was not as extensive as in the references, which indicates that the residual acetyl groups in the samples continue to provide a bulking effect. No rapid increase in MC_{CW}^* was seen in the WPG-18 samples in the early stages of decay, which suggests that the water capacity of the cell walls is less affected by deacetylation than hygroscopicity. The fact that *R. placenta* caused high mass losses even in the WPG-18 samples without extensive deacetylation shows that the fungus can degrade wood with reduced hygroscopicity and cell wall space.

Supplementary Information

The online version contains supplementary material available at https://doi.org/10.1186/s40712-025-00228-5.

Additional file 1: Figs. S1–S4

Acknowledgements
Not applicable.

Authors' contributions
Tiina Belt: conceptualisation; funding acquisition; investigation; methodology; resources; visualisation; writing—original draft; writing—review and editing; Michael Altgen: investigation; methodology; writing—review and editing.

Funding
This work received funding from the Research Council of Finland (grant no. 330087 and 349198).

Data availability
The datasets generated during the current study are available in the Zenodo repository, https://doi.org/https://doi.org/10.5281/zenodo.14177699.

Declarations

Ethics approval and consent to participate
Not applicable.

Competing interests
The authors declare that they have no competing interests.

Received: 12 December 2024 Accepted: 2 February 2025
Published online: 12 February 2025

References

Alfredsen G, Flæte PO, Militz H (2013) Decay resistance of acetic anhydride modified wood: a review. Int Wood Prod J 4:137–143. https://doi.org/10.1179/2042645313Y.0000000034

Arantes V, Goodell B (2014) Current understanding of brown-rot fungal biodegradation mechanisms: a review. In: Schultz TP, Goodell B, Nicholas DD (eds) Deterioration and Protection of Sustainable Biomaterials. American Chemical Society, Washing, DC

Awais M, Altgen M, Belt T, Teräväinen V, Mäkelä M, Altgen D, Nopens M, Rautkari L (2022) Wood–water relations affected by anhydride and formaldehyde modification of wood. ACS Omega 7:42199–42207. https://doi.org/10.1021/acsomega.2c04974

Beck G, Hegnar OA, Fossdal CG, Alfredsen G (2018a) Acetylation of Pinus radiata delays hydrolytic depolymerisation by the brown-rot fungus Rhondonia placenta. Int Biodeter Biodegrad 135:39–52. https://doi.org/10.1016/j.ibiod.2018.09.003

Beck G, Thybring EE, Thygesen LG (2018b) Brown-rot fungal degradation and de-acetylation of acetylated wood. Int Biodeter Biodegrad 135:62–70. https://doi.org/10.1016/j.ibiod.2018.09.009

Beck G, Thybring EE, Thygesen LG, Hill C (2018c) Characterization of moisture in acetylated and propionylated radiata pine using low-field nuclear magnetic resonance (LFNMR) relaxometry. Holzforschung 72:225–233. https://doi.org/10.1515/hf-2017-0072

Belt T, Awais M (2025) Progressive degradation of acetylated wood by the brown rot fungi Coniophora puteana and Rhodonia placenta. Wood Sci Technol 59:13. https://doi.org/10.1007/s00226-024-01620-8

Belt T, Altgen M, Awais M, Nopens M, Rautkari L (2024) Degradation by brown rot fungi increases the hygroscopicity of heat-treated wood. Int Biodeter Biodegrad 186:105690. https://doi.org/10.1016/j.ibiod.2023.105690

Čermák P, Baar J, Dömény J, Výbohová E, Rousek R, Pařil P, Oberle A, Čabalová I, Hess D, Vodák M, Brabec M (2022) Wood-water interactions of thermally modified, acetylated and melamine formaldehyde resin impregnated beech wood. Holzforschung 76:437–450. https://doi.org/10.1515/hf-2021-0164

Curling SF, Clausen CA, Winandy JE (2002) Relationships between mechanical properties, weight loss, and chemical composition of wood during incipient brown-rot decay. Forest Prod J 52:6

Daniel G (2014) Fungal and bacterial biodegradation: white rots, brown rots, soft rots, and bacteria. In: Schultz TP, Goodell B, Nicholas DD (eds) Deterioration and Protection of Sustainable Biomaterials. American Chemical Society, Washing, DC

Digaitis R, Thybring EE, Thygesen LG, Fredriksson M (2021) Targeted acetylation of wood: a tool for tuning wood-water interactions. Cellulose 8009–8025. https://doi.org/10.1007/s10570-021-04033-z
Fengel D, Wegener G (1989) Wood: chemistry, ultrastructure, reactions. Walter de Gruyter, Berlin
Filley TR, Cody GD, Goodell B, Jellison J, Noser C, Ostrofsky A (2002) Lignin demethylation and polysaccharide decomposition in spruce sapwood degraded by brown rot fungi. Org Geochem 33:111–124. https://doi.org/10.1016/S0146-6380(01)00144-9
Flournoy DS, Kirk TK, Highley TL (1991) Wood decay by brown-rot fungi: changes in pore structure and cell wall volume. Holzforschung 45:383–388. https://doi.org/10.1515/hfsg.1991.45.5.383
Fredriksson M, Digaitis R, Engqvist J, Thybring EE (2023) Effect of targeted acetylation on wood–water interactions at high moisture states. Cellulose. https://doi.org/10.1007/s10570-023-05678-8
Glass SV, Boardman CR, Thybring EE, Zelinka SL (2018) Quantifying and reducing errors in equilibrium moisture content measurements with dynamic vapor sorption (DVS) experiments. Wood Sci Technol 52:909–927. https://doi.org/10.1007/s00226-018-1007-0
Goodell B, Zhu Y, Kim S, Kafle K, Eastwood D, Daniel G, Jellison J, Yoshida M, Groom L, Pingali SV, O'Neill H (2017) Modification of the nanostructure of lignocellulose cell walls via a non-enzymatic lignocellulose deconstruction system in brown rot wood-decay fungi. Biotechnol Biofuels 10:179. https://doi.org/10.1186/s13068-017-0865-2
Hammel KE, Kapich AN, Jensen KA, Ryan ZC (2002) Reactive oxygen species as agents of wood decay by fungi. Enzyme Microb Technol 30:445–453. https://doi.org/10.1016/S0141-0229(02)00011-X
Hill CAS, Forster SC, Farahani MRM, Hale MDC, Ormondroyd GA, Williams GR (2005) An investigation of cell wall micropore blocking as a possible mechanism for the decay resistance of anhydride modified wood. Int Biodeter Biodegrad 55:69–76. https://doi.org/10.1016/j.ibiod.2004.07.003
Hill CAS, Hale MD, Ormondroyd GA, Kwon JH, Forster SC (2006) Decay resistance of anhydride-modified Corsican pine sapwood exposed to the brown rot fungus Coniophora puteana. Holzforschung 60:625–629. https://doi.org/10.1515/HF.2006.105
Himmel S, Mai C (2015) Effects of acetylation and formalization on the dynamic water vapor sorption behavior of wood. Holzforschung 69:633–643. https://doi.org/10.1515/hf-2014-0161
Kyyrö S, Altgen M, Seppäläinen H, Belt T, Rautkari L (2021) Effect of drying on the hydroxyl accessibility and sorption properties of pressurized hot water extracted wood. Wood Sci Technol. https://doi.org/10.1007/s00226-021-01307-4
Papadopoulos AN, Hill CAS (2003) The sorption of water vapour by anhydride modified softwood. Wood Sci Technol 37:221–231. https://doi.org/10.1007/s00226-003-0192-6
Ponzecchi A, Alfredsen G, Fredriksson M, Thybring EE, Thygesen LG (2024) Localization and characterisation of brown rot in two types of acetylated wood. Cellulose 1875–1890. https://doi.org/10.1007/s10570-023-05680-0
Popescu C-M, Hill CAS, Curling S, Ormondroyd G, Xie Y (2014) The water vapour sorption behaviour of acetylated birch wood: how acetylation affects the sorption isotherm and accessible hydroxyl content. J Mater Sci 49:2362–2371. https://doi.org/10.1007/s10853-013-7937-x
Ringman R, Pilgård A, Brischke C, Richter K (2014) Mode of action of brown rot decay resistance in modified wood: a review. Holzforschung 68:239–246. https://doi.org/10.1515/hf-2013-0057
Ringman R, Beck G, Pilgård A (2019) The importance of moisture for brown rot degradation of modified wood: a critical discussion. Forests 10:522. https://doi.org/10.3390/f10060522
Sandberg D, Kutnar A, Karlsson O, Jones D (2021) Wood modification technologies: principles, sustainability, and the need for innovation. CRC Press - Taylor & Francis, Boca Raton
Thybring EE (2013) The decay resistance of modified wood influenced by moisture exclusion and swelling reduction. Int Biodeter Biodegrad 82:87–95. https://doi.org/10.1016/j.ibiod.2013.02.004
Thybring EE, Kymäläinen M, Rautkari L (2018) Experimental techniques for characterising water in wood covering the range from dry to fully water-saturated. Wood Sci Technol 52:297–329. https://doi.org/10.1007/s00226-017-0977-7
Thybring EE, Digaitis R, Nord-Larsen T, Beck G, Fredriksson M (2020a) How much water can wood cell walls hold? A triangulation approach to determine the maximum cell wall moisture content. PLoS ONE 15:e0238319. https://doi.org/10.1371/journal.pone.0238319
Thybring EE, Piqueras S, Tarmian A, Burgert I (2020b) Water accessibility to hydroxyls confined in solid wood cell walls. Cellulose 27:5617–5627. https://doi.org/10.1007/s10570-020-03182-x
Thygesen LG, Engelund ET, Hoffmeyer P (2010) Water sorption in wood and modified wood at high values of relative humidity. Part I: Results for untreated, acetylated, and furfurylated Norway spruce. Holzforschung 64:315–323. https://doi.org/10.1515/hf.2010.044
Thygesen LG, Beck G, Nagy NE, Alfredsen G (2021) Cell wall changes during brown rot degradation of furfurylated and acetylated wood. Int Biodeter Biodegrad 162:105257. https://doi.org/10.1016/j.ibiod.2021.105257
Yelle DJ, Wei D, Ralph J, Hammel KE (2011) Multidimensional NMR analysis reveals truncated lignin structures in wood decayed by the brown rot basidiomycete Postia placenta. Environ Microbiol 13:1091–1100. https://doi.org/10.1111/j.1462-2920.2010.02417.x
Zelinka SL, Ringman R, Pilgård A, Thybring EE, Jakes JE, Richter K (2016) The role of chemical transport in the brown-rot decay resistance of modified wood. Int Wood Prod J 7:66–70. https://doi.org/10.1080/20426445.2016.1161867
Zelinka SL, Glass SV, Lazarcik EQD, Thybring EE, Altgen M, Rautkari L, Curling S, Cao J, Wang Y, Künniger T, Nyström G, Dreimol CH, Burgert I, Uyup MKA, Khadiran T, Roper MG, Broom DP, Schwarzkopf M, Yudhanto A, Subah M, Lubineau G, Fredriksson M, Strojecki M, Olek W, Majka J, Pedersen NB, Burnett DJ, Garcia AR, Verdonck E, Dreisbach F, Waguespack L, Schott J, Esteban LG, Garcia-Iruela A, Colinart T, Rémond R, Mazian B, Perre P, Emmerich L, Li L (2024) Interlaboratory study of the operational stability of automated sorption balances. Adsorption. https://doi.org/10.1007/s10450-024-00472-9
Zhu Y, Li W, Meng D, Li X, Goodell B (2022) Non-enzymatic modification of the crystalline structure and chemistry of Masson pine in brown-rot decay. Carbohydr Polym 286:119242. https://doi.org/10.1016/j.carbpol.2022.119242

Publisher's Note